Optics Communications 503 (2022) 127459

Contents lists available at ScienceDirect

Optics Communications

journal homepage: www.elsevier.com/locate/optcom

Polarization-insensitive dielectric metamaterial absorber for near-unity UV-light trapping in monolayer graphene

Yinong Xie [a,b], Xueying Liu [a,b], Yijun Cai [c,*], Jinfeng Zhu [a,b,*]

[a] Institute of Electromagnetics and Acoustics, Xiamen University, Xiamen 361005, China
[b] State Key Laboratory of Applied Optics, Changchun Institute of Optics, Fine Mechanics and Physics, Chinese Academy of Sciences, Changchun 130033, China
[c] Fujian Provincial Key Laboratory of Optoelectronic Technology and Devices, Xiamen University of Technology, Xiamen 361024, China

ARTICLE INFO

Keywords:
Dielectric metamaterial
UV-light trapping
Monolayer graphene
Polarization-insensitive

ABSTRACT

With the aim of improving UV light trapping capability in monolayer graphene, a nanomesh metamaterial absorber is proposed, which exhibits the polarization-insensitive feature due to the geometrical symmetry. Through the functional combination of magnetic resonance and UV mirror, the absorption of unpolarized UV light in monolayer graphene can reach 99.5% under normal incidence. The absorption enhancement is induced by the magnetic resonance mode between the dielectric silica nanomesh and the calcium fluoride base layer. The effects of geometric parameters on the absorption spectra are systematically investigated. The proposed structure shows insensitive to manufacturing deviations, which can maintain at a high UV absorption rate of more than 99% within the nanomesh width ranging from 50 nm to 90 nm. Furthermore, after delicate optimization of the geometric parameters, two sharp resonances with absorbance more than 90% can be excited simultaneously inside the absorber. Our work provides an important theoretical guide for the design of optoelectronic devices based on two-dimensional materials in the UV range.

1. Introduction

In recent years, graphene has become one of the most popular two-dimensional (2D) materials from UV to terahertz ranges due to its fast and broadband optical response [1–5], high carrier mobility, extraordinary band structure, and unique mechanical strength and flexibility [6–9]. Within the spectral range from mid-infrared to terahertz, graphene supports a robust plasmonic response, which significantly enhances the light-graphene interaction. However, in the range from UV to near-infrared (NIR), due to the absence of plasmonic response, monolayer graphene can only absorb a very tiny fraction of the normal incident light (~2.3% for the visible–NIR range, and less than 9% for the UV range [10,11]). Several studies have used graphene with multiple atomic layers to improve the absorption efficiency. However, the superior performance of graphene as a 2D material will undoubtedly degrade, such as photonic and electron conduction efficiencies [12–14].

Therefore, numerous methods have been intensively studied to strengthen the interaction between monolayer graphene and the incident light, such as configurations with subwavelength-scale patterning inside graphene layers [15,16]. Nevertheless, they will not only makes manufacturing more complicated and expensive, but also cause irreversible damage to the electronic and photonic properties of monolayer graphene, whose band structure is very sensitive to atom-scale damage and environmental contaminant.

Unlike the conventional studies from visible to terahertz spectrum range, the many-body effects of graphene should be taken into account for the high excitation energy of UV light [17]. Graphene and metals in the UV band exhibit totally different properties from those in the longer wavelength range. It might be much more difficult for precise fabrication of nanoscale features applied on graphene with shorter wavelength range, thus a series of new material and structural engineering which can be learned from other fields are required for trapping UV light in the unpatterned monolayer graphene [18–20]. A previous study has achieved high optical absorption in graphene by using an unpatterned graphene/medium/metal structure [21]. However, the configuration required specific angle control and polarization manipulation for the incident light.

In order to increase the absorption efficiency of UV light in graphene under normal incidence, plasmonic devices based on periodic Al nanostructured arrays have been developed to excite the plasmon within the UV spectral range [22,23]. Unfortunately, most of the incident energy is dissipated in the lossy Al due to the considerable inherent loss of metal. Several periodic dielectric grating arrays are used to trap light for total absorption. However, these efforts mainly focused on the infrared range and require additional polarization manipulation [24,25]. Therefore, a metamaterial absorber for enhancing UV light-graphene interaction with polarization-insensitive property is quite in demand.

* Corresponding authors.
E-mail addresses: yijuncai@foxmail.com (Y. Cai), nanoantenna@hotmail.com (J. Zhu).

https://doi.org/10.1016/j.optcom.2021.127459
Received 15 June 2021; Received in revised form 12 September 2021; Accepted 14 September 2021
Available online 17 September 2021

In this work, we propose a graphene-based UV metamaterial absorber with near-unity optical absorption inside graphene. It consists of all-dielectric materials except for graphene and possesses the characteristic of polarization independence. We conduct a systematic investigation on the geometric design, material selection, and polarization properties for the configuration of proposed absorber in the UV band. After rigorous structural optimization, the absorption of UV light inside graphene can be increased up to 99.5%, which is more than 10 times larger than that inside suspended graphene. Moreover, the electric and magnetic field distributions are investigated to reveal the absorption mechanism.

2. Structural design and numerical simulations

The schematic illustration of the all-dielectric photonic structure is exhibited in Fig. 1, which shows that the central symmetric silicon dioxide (SiO_2) nanomesh is prepared on the surface of the calcium fluoride (CaF_2) layer. Then the monolayer graphene as the absorption material is transferred and sandwiched between them. The laminated structure with almost perfect reflection is formed by the dielectric layer with a high refractive index layer (ZrO_2) and low refractive index (Na_3AlF_6), while the transparent substrate (SiO_2) also acts as a part of the UV mirror. The geometry of the metamaterial is described by t_1, w, t_2, and p as shown in Fig. 1. The numerical simulation is conducted by the commercial software COMSOL Multiphysics. The periodic boundary conditions are adopted in the x-axis and y-axis, respectively. The normal incident light is introduced from above along z-axis direction. In our design, the dielectric layers of SiO_2, CaF_2, ZrO_2, Na_3AlF_6 and substrate are assumed to be nonmagnetic ($\mu = \mu_0$) and optically lossless with the refractive index of 1.48, 1.45, 2.60, 1.33 and 1.48, respectively. The UV mirror is optimized with 5 layers of ZrO_2 (26.9 nm thick) and 4 layers of Na_3AlF_6(52.6 nm thick) for nearly-total reflection under normal incidence. Based on the many-body effects in the UV range, monolayer graphene could be considered as a 2D conductive surface with a dispersive conductivity σ, which can be described by the equations of the Fano model [26],

$$\sigma(\lambda) = \frac{\sigma_{CB}(\lambda) \cdot (q + \varepsilon)}{1 + \varepsilon^2} \tag{1}$$

$$\varepsilon = \frac{h_C/\lambda - E_r}{\Gamma/2} \tag{2}$$

where λ, h_c and c represent the free space wavelength, Planck constant and the speed of light in vacuum, respectively. $\sigma_{CB}(\lambda)$ is the continuum background from the calculation of a many-body system, which represents the response away from the singularity [27]. The Fano parameter $q = -1$ denotes the intensity of the excitonic transition to the unperturbed band transitions and the asymmetry of the conductivity line shape. ϵ is the normalized energy by width Γ=0.78 eV relative to the resonance energy $E_r = 5.02$ eV of the perturbed exciton. Optical simulations are performed to optimize the parameters of the structure for complete UV light absorption.

3. Results and discussion

Initially, we investigate the polarization dependence of incident light by comparing the absorbance of nanograting and nanomesh structures under *s*-polarized and *p*-polarized incidence, respectively, as shown in Fig. 2(a) (the schematic drawings of the two structures are shown in the inset). The nanograting structure exhibits relatively high absorbance under *s*-polarized incidence, while the absorbance is rather low under *p*-polarized light incidence, which indicates obvious polarization dependence. In contrast, the nanomesh structure with the same geometric parameters has a relatively high UV absorbance inside graphene for both *s*-polarized and *p*-polarized incidence, which is attributed to the central symmetry of the nanomesh structure. The maximum UV absorbance peak is larger than 80% at $\lambda = 273$ nm and the absorbance spectra of the two polarizations are identical, which solves

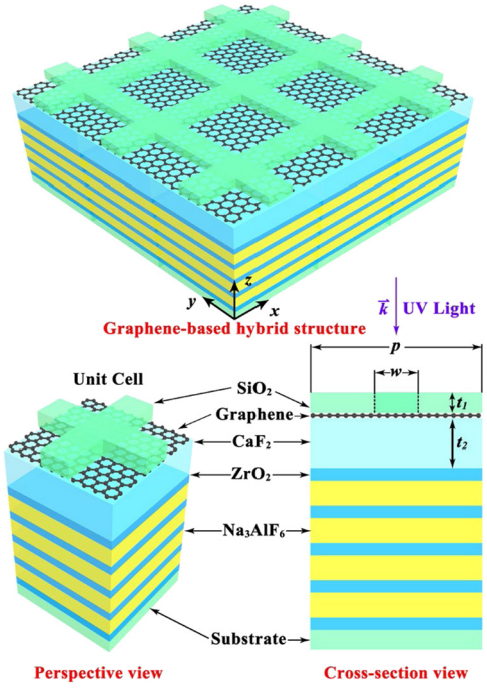

Fig. 1. Schematic drawing of the proposed UV absorber based on graphene. The symbols w, p, t_1 and t_2 represent the width of nanomesh, period of nanomesh, thickness of silica nanomesh layer and thickness of CaF_2, respectively.

the problem of polarization dependence of the nanograting structure. Moreover, as shown in Fig. 2(b), owing to the polarization dependence of grating structure, the absorbance inside graphene is only 65% at 273 nm under unpolarized incidence. In order to reveal the mechanism of the absorption enhancement, the magnetic field and electric field distributions of the nanomesh structure are plotted in Fig. 2(c) and Fig. 2(d). A remarkable magnetic dipole resonance appears around the graphene layer at $\lambda = 273$ nm while the off-resonance state is observed at $\lambda = 332$ nm. For an optimized structure, the presence of magnetic resonance induces the concentrated electric field parallel to the graphene layer and contributes to the enhanced UV absorption inside graphene as shown in Fig. 2(d). This phenomenon can be further explained by t he quantitatively calculation of optical absorption. In graphene, the optical absorption is determined by the following equation [28],

$$A(\lambda) = \frac{4\pi c}{\lambda} \cdot n(\lambda) \cdot k(\lambda) \cdot \int_V |E_l|^2 \, dV \tag{3}$$

where c and λ are the speed and wavelength of light in free space, V is the volume of graphene, and E_l is the local electric field. Based on Eq. (3), the absorbance is proportional to the square of local electric field intensity. Apparently, the absorbance of UV light inside graphene is significantly improved at $\lambda = 273$ nm due to the strong enhancement of in-plane electric field.

We next consider the influence of the SiO_2 layer thickness on the UV absorption. As t_1 increases from 10 nm to 150 nm as shown in Fig. 3(a), the UV absorbance peak exhibits a redshift from 268 nm to 282 nm due to the increment of the effective resonant wavelength of the magnetic dipole. When t_1 is set at a low value of 10 nm, the maximum absorbance is relatively low, which is due to the confinement of the magnetic resonance mode (MRM) inside the CaF_2 layer while the corresponding electric field enhancement is intensively concentrated in this layer. As shown in Fig. 3(b), when $t_1 = 30$ nm, MRM is obviously changed due to the much stronger in-plane electric field concentration on the graphene surface compared with $t_1 = 10$ nm. Along with the further increase of t_1, there is an optimum value of 100 nm. As shown in Fig. 3(b) when

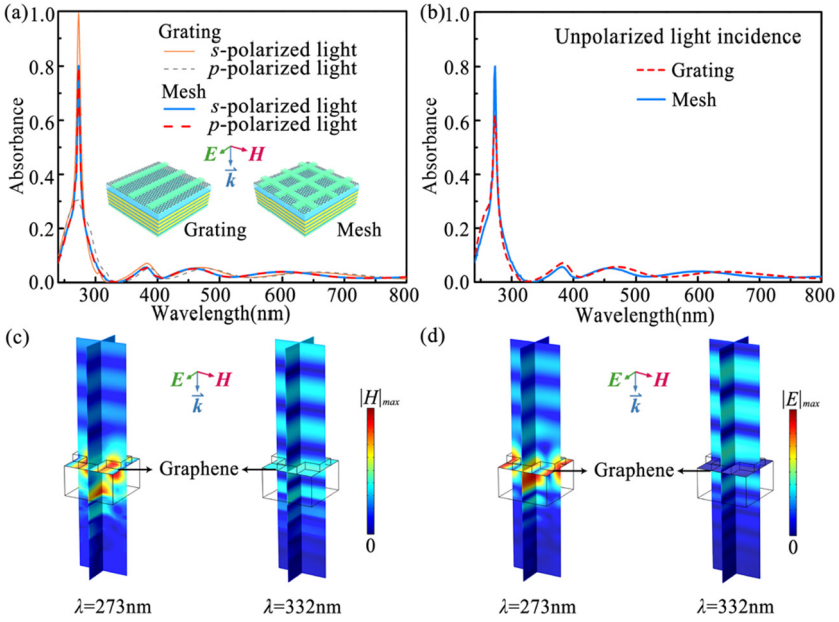

Fig. 2. (a) Comparison of absorbance between nanograting and nanomesh structures under different polarizations. (b) Comparison of absorbance between nanograting and nanomesh structures for unpolarized light. (c) Magnetic field distributions and (d) Electric field distributions for $w = 111$ nm, $p = 220$ nm, $t_1 = 30$ nm and $t_2 = 120$ nm.

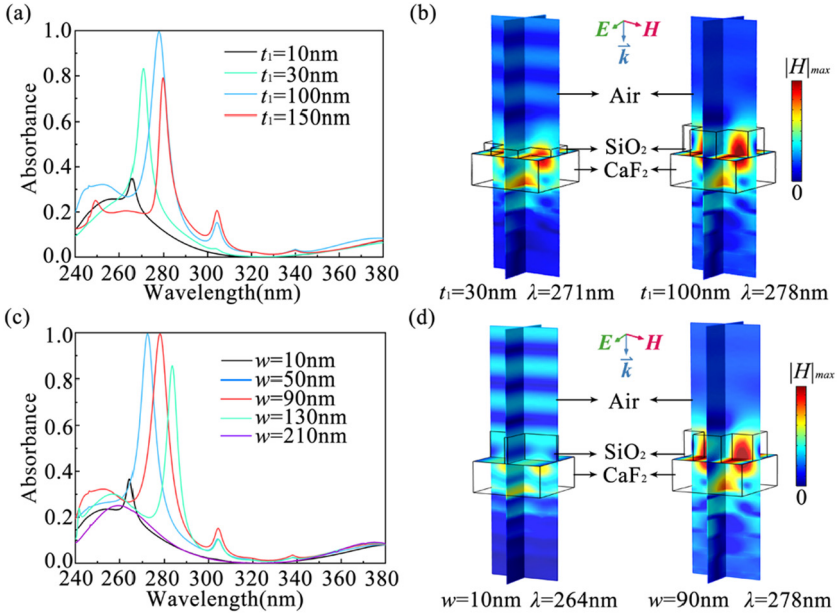

Fig. 3. (a) Absorbance of graphene as a function of λ and t_1, where $p = 220$ nm, $w = 90$ nm and $t_2 = 120$ nm. (b) Comparison of magnetic field distributions under different t_1 for $p = 220$ nm, $w = 90$ nm and $t_2 = 120$ nm. (c) Absorbance in graphene as a function of λ and w, where $p = 220$ nm, $t_1 = 100$ nm and $t_2 = 120$ nm. (d) Comparison of magnetic field distributions under different w for $p = 220$ nm, $t_1 = 100$ nm and $t_2 = 120$ nm.

$t_1 = 100$ nm, the in-plane electric field induced by the MRM is highly confined on the graphene surface leading to the highest UV absorption of 99.5% at $\lambda = 278$ nm. As t_1 changes to 150 nm, the MRM moves gradually away from the surrounding environment of graphene surface, which leads to the decrease of maximum UV absorption rate.

We further consider the effect of w variation on the absorption of graphene, as demonstrated in Fig. 3(c). In this discussion, the period is fixed at $p = 220$ nm. As w increases from 10 nm to 130 nm, the maximum absorption peak shifts from 264 nm to 284 nm. When the filling factor determined by w/p is small enough ($w = 10$ nm), the intensity of the localized electric field parallel to the graphene surface is relatively weak, which leads to an insufficient absorption enhancement. This is mainly because the MRM cannot be effectively excited due to the tiny filling factor as shown in Fig. 3(d). As w becomes larger, the electric field mode is obviously enhanced, resulting in a significant increase of absorbance. For the width ranging from 50 nm to 90 nm, the maximum absorbance ratios remain above 99%. As w is set as the optimized value of 90 nm, the obvious MRM leads to the significant concentration and enhancement of in-plane electric field in the graphene surface, then a near-unity absorption is achieved at $\lambda = 278$ nm. As w increases and approaches p, the filling factor w/p is almost equal to 1. Electric fields cannot be concentrated due to the attenuation of MRM in the nanostructure, resulting in the dramatic reduction of UV absorption.

After discussing the effects of the thickness and width of SiO_2 layer, we investigate the influence of the nanostructure period p and the

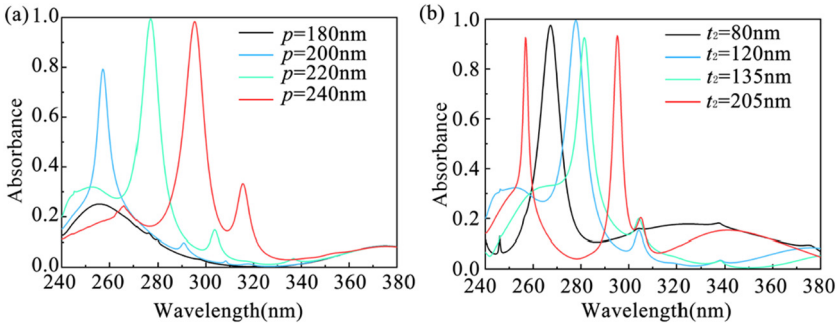

Fig. 4. Absorbance in graphene as a function of λ and p, where $w = 90$ nm, $t_1 = 100$ nm and $t_2 = 120$ nm. (b). Absorbance in graphene as a function of λ and t_2, where $p = 220$ nm, $t_1 = 100$ nm and $t_2 = 120$ nm.

CaF_2 thickness t_2 on the UV absorption as demonstrated in Fig. 4. As shown in Fig. 4(a), when p is chosen as 180 nm, the MRM cannot be effectively excited, resulting in a relatively low absorbance. With the increase of p, the MRM is excited and strengthened, while the absorption rate increases dramatically. The MRM is not completely excited until p increases to 220 nm. Meanwhile, the maximum in-plane field on the graphene surface is induced, which results in the corresponding maximum absorption rate of 99.5% at $\lambda = 278$ nm. With the further increase of p, the absorption peak has a redshift and the absorbance slightly drops down. These results indicate that there is an optimum value of the period for the maximum UV absorption.

We finally study the influence of CaF_2 thickness on the UV absorption spectrum. As shown in Fig. 4(b), when t_2 changes from 80 nm to 135 nm, the resonant wavelength has a redshift from 262 nm to 282 nm. The red-shifted range is significantly larger than that caused by the change of t_1 originating from the fact that the resonance has a dominant mode region in the CaF_2 layer. Accordingly, the change of t_2 seriously affects the absorption enhancement caused by the interference. Particularly, when t_2 reaches 205 nm, the absorption enhancement caused by interference can even be comparable to the absorption peak of magnetic resonance, resulting in dual absorption peaks in the UV band. It provides a new way for the application of UV double resonance spectroscopy [29,30].

4. Conclusion

In summary, we propose a polarization-independent near-unity metamaterial absorber in the UV range based on the monolayer graphene. The use of all-dielectric materials avoids the intrinsic loss inside metal materials. Meanwhile, the existence of the UV mirror leads to a higher reflection rate of UV light and more energy loss inside monolayer graphene. Due to the electric field enhancement caused by magnetic dipole resonance in monolayer graphene, an optimized metamaterial absorber can achieve a UV absorption rate up to 99.5%. Besides, it reveals an excellent polarization-insensitive property due to the geometrical symmetry, which brings more convenience in light path construction and device integration of UV absorption. In addition, by adjusting the thickness of the CaF_2 layer and the period of the unit cell properly, double resonances with absorption rates more than 90% can be observed in the spectrum. The proposed absorber greatly enhances the light-matter interaction for near-unity UV absorption in sub-nanometer 2D materials, which has a great potential for the development of high-performance optoelectronic devices in the UV range.

Declaration of competing interest

The authors declare that they have no known competing financial interests or personal relationships that could have appeared to influence the work reported in this paper.

Acknowledgments

This work was financially supported by National Natural Science Foundation of China (U1830116, 62005232); the Open Fund of State Key Laboratory of Applied Optics (SKLAO2020001A15); Fundamental Research Funds for the Central Universities (20720190010); Natural Science Foundation of Fujian Province (2020J01294); Xiamen Science and Technology Bureau (3502Z20203006).

References

[1] R. Tang, S. Han, F. Teng, K. Hu, Z. Zhang, M. Hu, X. Fang, Size-controlled graphene nanodot arrays/ZnO hybrids for high-performance UV photodetectors, Adv. Sci. 5 (2018) 1700334.
[2] L. Ye, Y. Chen, G. Cai, N. Liu, J. Zhu, Z. Song, Q.H. Liu, Broadband absorber with periodically sinusoidally-patterned graphene layer in terahertz range, Opt. Express 25 (2017) 11223–11232.
[3] T. Chen, Y. Lu, Y. Sheng, Y. Shu, X. Li, R. Chang, H. Bhaskaran, J.H. Warner, Ultrathin all-2D lateral Graphene/GaS/Graphene UV photodetectors by direct CVD growth, Acs Appl. Mater. Inter. 11 (2019) 48172–48178.
[4] I.H. Lee, D. Yoo, P. Avouris, T. Low, S.H. Oh, Graphene acoustic plasmon resonator for ultrasensitive infrared spectroscopy, Nat. Nanotechnol. 14 (2019) 313–319.
[5] J. Zhu, C. Li, J.Y. Ou, Q.H. Liu, Perfect light absorption in graphene by two unpatterned dielectric layers and potential applications, Carbon 142 (2019) 430–437.
[6] J. Wang, Y. Hernandez, M. Lotya, J.N. Coleman, W.J. Blau, Broadband nonlinear optical response of graphene dispersions, Adv. Mater. 21 (2009) 2430–2435.
[7] D.B. Farmer, H.Y. Chiu, Y.M. Lin, K.A. Jenkins, F. Xia, P. Avouris, Utilization of a buffered dielectric to achieve high field-effect carrier mobility in graphene transistors, Nano Lett. 9 (2009) 4474–4478.
[8] M.I. Katsnelson, K.S. Novoselov, Graphene: New bridge between condensed matter physics and quantum electrodynamics, Solid State Commun. 143 (2007) 3–13.
[9] Q. Bao, K.P. Loh, Graphene photonics, plasmonics, and broadband optoelectronic devices, ACS Nano. 6 (2012) 3677–3694.
[10] R.R. Nair, P. Blake, A.N. Grigorenko, K.S. Novoselov, T.J. Booth, T. Stauber, N.M.R. Peres, A.K. Geim, Fine structure constant defines visual transparency of graphene, Science 320 (2008) 1308.
[11] S. Bae, H. Kim, Y. Lee, X. Xu, J. Park, Y. Zheng, J. Balakrishnan, T. Lei, H.R. Kim, Y. Song II, Y. Kim, K.S. Kim, B.O. zyilmaz, J. Ahn, B.H. Hong, S. Iijima, Roll-to-roll production of 30-inch graphene films for transparent electrodes, Nat. Nanotechnol. 5 (2010) 574.
[12] M. Koshino, Stacking-dependent optical absorption in multilayer graphene, New J. Phys. 15 (2013) 015010.
[13] M. Koshino, T. Ando, Electronic structures and optical absorption of multilayer graphenes, Solid State Commun. 149 (2009) 1123–1127.
[14] P.A. Obraztsov, M.G. Rybin, A.V. Tyurnina, S.V. Garnov, E.D. Obraztsova, A.N. Obraztsov, Y.P. Svirko, Broadband light-induced absorbance change in multilayer graphene, Nano Lett. 11 (2011) 1540–1545.
[15] C. Berger, Z. Song, X. Li, X. Wu, N. Brown, C. Naud, D. Mayou, T. Li, J. Hass, A.N. Marchenkov, E.H. Conrad, P.N. First, E.H. Conrad, Electronic confinement and coherence in patterned epitaxial graphene, Science 312 (2006) 1191–1196.
[16] H. Ago, I. Tanaka, C.M. Orofeo, M. Tsuji, K.I. Ikeda, Patterned growth of graphene over epitaxial catalyst, Small 6 (2010) 1226–1233.
[17] J. Zhou, S. Yan, C. Li, J. Zhu, Q.H. Liu, Perfect ultraviolet absorption in graphene using the magnetic resonance of an all-dielectric nanostructure, Opt. Express 26 (2018) 18155–18163.

[18] Y.I. Abdulkarim, F.Ö. Alkurtc, H.N. Awl, F.F. Muhammadshari, M. Bakırf, S. Dalgacg, M. Karaaslanc, H. Luo, An ultrathin and dual band metamaterial perfect absorber based on ZnSe for the polarization-independent in terahertz range, Results Phys. 26 (2021) 104344.
[19] M.Ç. Ayan, S. Kiri̧ s, A. Yapici, M. Karaaslan, O. Akgöl, O. Altınta̧ s, E. Ünal, Investigation of cotton fabric composites as a natural radar-absorbing material, Aircr. Eng. Aerosp. Technol. 92 (2020) 1275–1280.
[20] M. Sağık, M. Karaaslan, E. Ünal, O. Akgöl, M. Bakır, V. Akdogan, E. Özdemir, Y.I. Abdulkarim, C-shaped split ring resonator type metamaterial antenna design using neural network, Opt. Eng. 60 (2021) 1–14.
[21] J. Zhu, S. Yan, N. Feng, L. Ye, J.Y. Ou, Q.H. Liu, Near unity ultraviolet absorption in graphene without patterning, Appl. Phys. Lett. 112 (2018) 153106.
[22] R. González-Campuzano, J.M. Saniger, D. Mendoza, Plasmonic resonances in hybrid systems of aluminum nanostructured arrays and few layer graphene within the UV–IR spectral range, Nanotechnology 28 (2017) 465704.
[23] Y. Cai, Z. Wang, S. Yan, L. Ye, J. Zhu, Ultraviolet absorption band engineering of graphene by integrated plasmonic structures, Opt. Mater. Express 8 (2018) 3295–3306.
[24] C. Guo, Z. Zhu, X. Yuan, W. Ye, K. Lliu, J. Zhang, W. Xu, S. Qin, Experimental demonstration of total absorption over 99% in the near infrared for monolayer-graphene-based subwavelength structures, Adv. Opt. Mater. 4 (2016) 1955–1960.
[25] Y. Qing, H. Ma, Y. Ren, S. Yu, T. Cui, Near-infrared absorption-induced switching effect via guided mode resonances in a graphene-based metamaterial, Opt. Express 27 (2019) 5253–5263.
[26] K.F. Mak, J. Shan, T.F. Heinz, Seeing many-body effects in single-and few-layer graphene: observation of two-dimensional saddle-point excitons, Phys. Rev. Lett. 106 (2011) 046401.
[27] L. Yang, J. Deslippe, C.H. Park, M.L. Cohen, S.G. Louie, Excitonic effects on the optical response of graphene and bilayer graphene, Phys. Rev. Lett. 103 (2009) 186802.
[28] Y. Cai, J. Zhu, Q.H. Liu, Tunable enhanced optical absorption of graphene using plasmonic perfect absorbers, Appl. Phys. Lett. 106 (2015) 043105.
[29] E.C. Stanca-Kaposta, J.P. Simonsm, High-resolution infrared-ultraviolet (IR–UV) double-resonance spectroscopy of biological molecules, in: Handbook of High-Resolution Spectroscopy, Wiley Online Library, 2011.
[30] M.P. Callahan, B. Crews, A. Abo-Riziq, L. Grace, M.S. de Vries, Z. Gengeliczki, T.M. Holmesc, G.A. Hill, IR–UV double resonance spectroscopy of xanthine, Phys. Chem. Chem. Phys. 9 (2007) 4587–4591.